Soft nanocrystalline alloys (Melt Spun)

Olivier Geoffroy

Institut Néel, CNRS - Université Joseph Fourier, BP 166, 38042 Grenoble cedex 9, France

1 Presentation

Nanocrystalline magnetic soft alloys were patented in 1987 [Yos 88] and can be seen as an extension of amorphous magnetic soft alloys, introduced towards 1970. There intrinsic extremely high magnetic permeability coupled with a low production cost allow to use them for a wide range of applications.

Different families exist with Typical composition (atomic) :

* $Fe_{73.5}Cu_1Nb_3Si_{15.5}B_7$ (***Finemet*** by Hitachi Metals, ***Vitroperm*** by Vacuumschmelze GmbH, † ***Nanophy*** by Imphy Alloys)
* $Fe(Co)_{86}Zr_7B_6Cu_1$ († ***Nanoperm*** by Alps Electric Co.)
* $(Fe_{1-x}Co_x)_{88}Hf_7B_4Cu_1$: ***Hitperm***

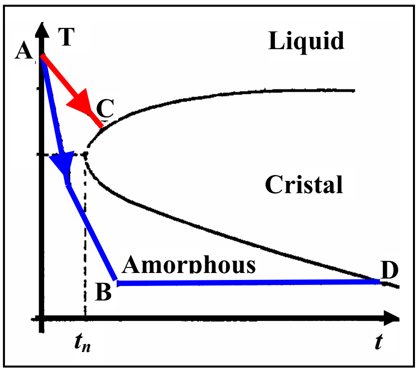

Fig. 1 : Temperature-duration-Transformation rate diagram

2 Elaboration and crystallographic structure

The elaboration is made of two stages :

* **First stage :** Elaboration of an amorphous precursor :
  - ➨ glass formers are needed (B, Hf…)
  - ➨ It is necessary to achieve very high cooling rate to prevent crystallisation (cf on fig 1 : route AB instead of route AC) :

$$\frac{dT}{dt} > 10^6 \text{ K / s}$$

  - ➨ Different technical processes exist :
  * Splat cooling (Not industrial) : compression of a liquid drop between two cooper disks.
  * Projection on a rotative cooled cooper wheel (Industrial) :
    - Melt spinning for ribbons of several millimetres width
    - Planar flow casting for ribbons of several centimetres width (until 20 cm)

* **Second stage :** Nanocristallisation annealing (≈ One hour, $T_{anneal} \approx 500$ °C)

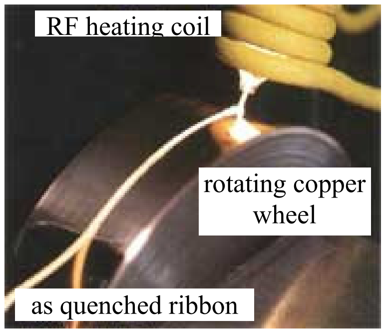

Fig. 2 a : melt spinning Process

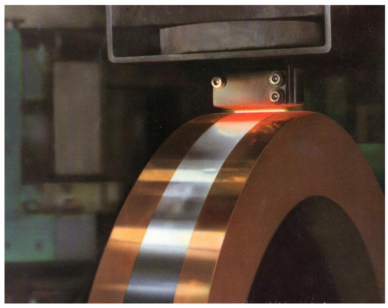

Fig. 2 b : Planar flow casting

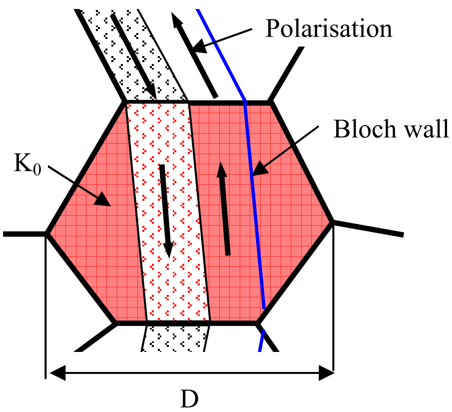

Fig. 3a : domain walls in classical crystalline alloys ($e_w \approx 3$ L << D)

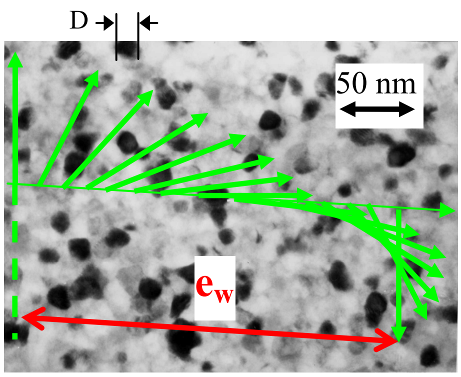

Fig. 3b : Microstructure of a Nanophy sample (Imphy Alloy). Superimposed, extension of a domain wall (thickness $e_w \approx 3$ L >> D)

- ➡ Rapid diffusion of Cu initiates local nucleation of crystalline FeSi (Finemet) or Fe (Nanoperm) with random crystallisation directions.
- ➡ Slow diffusion of Nb (Finemet) or Zr (Nanoperm) inhibs growth of crystallites : typical size $D \approx 10\text{-}20$ nm

➡ Atypical resulting crystalline structure (cf fig 3) :

Coexistence of a soft magnetic nanocristalline phase (Fe or FeSi) with a residual amorphous phase.
volumic crystalline fraction $f \approx 70$ %

3 Magnetic Properties

* Amorphous phase ensures continuity of magnetic exchanges interactions between nanograins :

- ➡ from a magnetic point of view, ribbon = continuous medium
- ➡ extension of a Domain-Wall upon a great number of grains ($e_w >> D$, cf. Figure 3b)
- ➡ At the scale of the DW, anisotropy K_{eff} much smaller than the crystallographic one K_0 due to averaging.

* In addition : very low magnetostriction (cf. fig.7) : $\lambda_s(f = 70\%) \approx 10^{-6}$

➡ Coercivity ↘↘ ($H_c < 1$ A/m)
Permeability ↗↗ ($\mu_r > 10^5$)

Quantitative description : **R**andom **A**nisotropy **M**odel

Magnetic independent entity = **C**orrelated **V**olume of side L (magnetic correlation length) (cf. fig. 4).

The effective anisotropy K_{eff} is driven by the random magnetocristalline contribution K_a. Noticing A the exchange stiffness, one obtains :

$$\left.\begin{array}{l} L = \sqrt{A\,K_{eff}} \\ K_{eff} = K_a = \sqrt{\langle K^2 \rangle} = K_0 / \sqrt{n} \\ n = f\,(L/D)^3 \end{array}\right\} K_{eff} \approx K_0^4\, A^{-3}\, f^{-2}\, D^6 \qquad (1)$$

$$H_c \approx K_{eff} \approx D^6 \quad \text{(cf. Fig.5)}$$

➡Related property :

Due to vanishing anisotropies, possibility to tailor the shape of the hysteretic loop by means of induced anisotropy

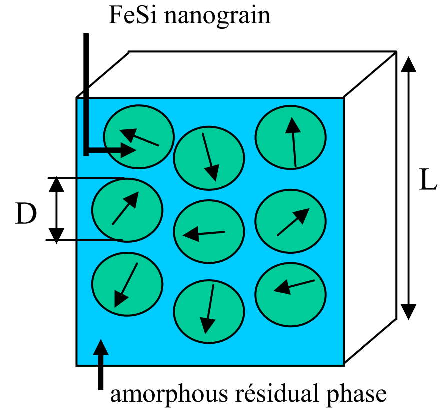

Fig. 4 : Magnetic correlated volume L^3 comprising $n = f\,(L/D)^3$ nanograins. Arrows feature the distribution of magnetization easy axes due to random cristallization

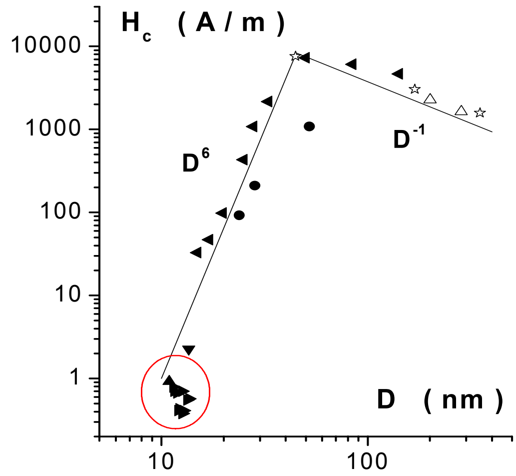

Fig. 5 : Evolution of the coercivity with the grain size. The D^{-1} dependancy corresponds to classical alloys ($e_w << D$, see fig.3a). The circle denotes the region where magnetoelastic effects have to be considered

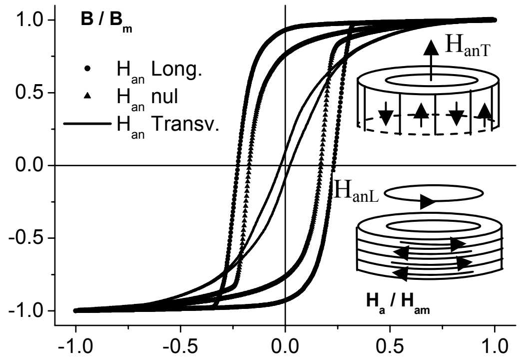

Fig. 6 : different shapes of the hysterical loop (round, flat, rectangular) obtained applying a magnetic field during annealing

applying stress or magnetic field during crystallisation annealing (cf fig. 6) [ALV 05]

4 Magnetostriction and Magnetoelastic effects :

For little grain sizes ($D \approx 10$ nm), deviation from the D^6 law occurs (cf. fig.5, circle) : in this region, **M**agneto**E**lastic effects give a significant contribution K_{me} to K_{eff}, leading instead of (1) to [SUS 98] :

$$K_{eff}^2 = K_{me}^2 + K_a^2 = K_{me}^2 + K_0^2 A^{-3/2} f^{-1} D^3 K_{eff}^{-3/2} \qquad (2)$$

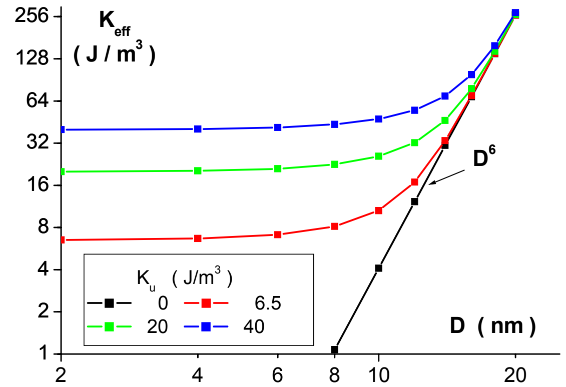

Fig. 7 : Modelisation of K_{eff} as a function of grains size for different valeues of K_u ($A = 10^{-11}$ J/m, f=1, $K_0 = 8000$ J/m^3)

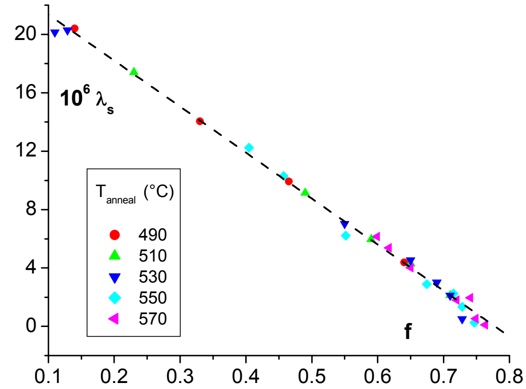

Fig. 8 : evolution of λ_s (measured by SAMR method) as a function of cristalline fraction f (samples Nanophy)

Figure 7 illustrates the competition between K_{me} and K_a. It is so expected that for little grain sizes H_c is controlled by the magnetostriction coeff. λ_s.

Measurements show that λ_s linearly depends on crystalline fraction f (cf. fig. 8) with, as a first approximation, the typical behaviour

$\lambda_s = f\,\lambda_c + (1\text{-}f)\,\lambda_a$

λ_c, λ_a = magnetostriction of crystalline and amorphous phases[1].

Starting from H_c, D, f, measurements, K_{me} is obtained from (2) and can be compared to λ_s measurements. With E = Young Modulus, it is experimentally obtained (cf. fig. 9)

$K_{me} = \alpha\, E\, \lambda_s^2 \qquad \alpha = 0{,}15$

The λ_s^2 dependency indicates that the source of stress is internal. Simple scaling argument explains that the source of Magnetoelastic frustration does not lie at the interface nanograin / amorphous but at the scale of the CV itself. According to quantitative modelisation [GEO 06], a reasonable scheme is that frustration occurs when the magnetization reverses in the CV : its shape (in black on Fig. 9) is imposed by the magnetization of the surrounding medium (black arrows), even when its own

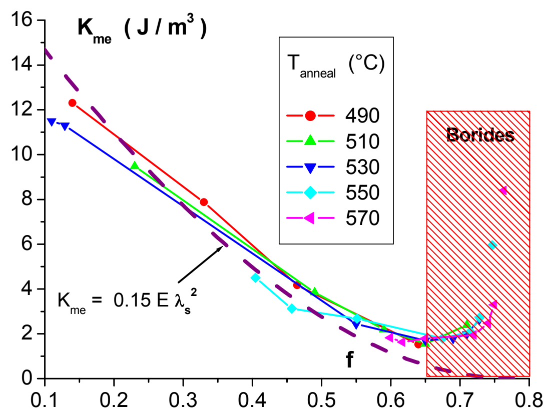

Fig. 9 : Evolution of K_{me} obtained from H_c measurements following (2) on Nanophy samples Comparison with a fit $\approx E\,\lambda_s^2$.

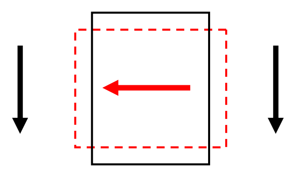

Fig. 10 : Schematic view of ME frustration occuring in CV at magnetisation reversal

---

[1] An accurate modelisation has to take into account the f dependance of λ_a due to change in the amorphous phase composition and the contribution of surface magnetostriction to λ_c in the little grain sizes range [SLA 98], [NAN 01], [SZU 02]

magnetization (red arrow) would promote the red shape (dash line).

5 Additional properties

* Ribbon thickness ≈ 20 µm
* Electrical resistivity $\rho \approx 140\ 10^{-8}\ \Omega$

} → Nanocristalline alloys = good candidates for medium frequencies applications

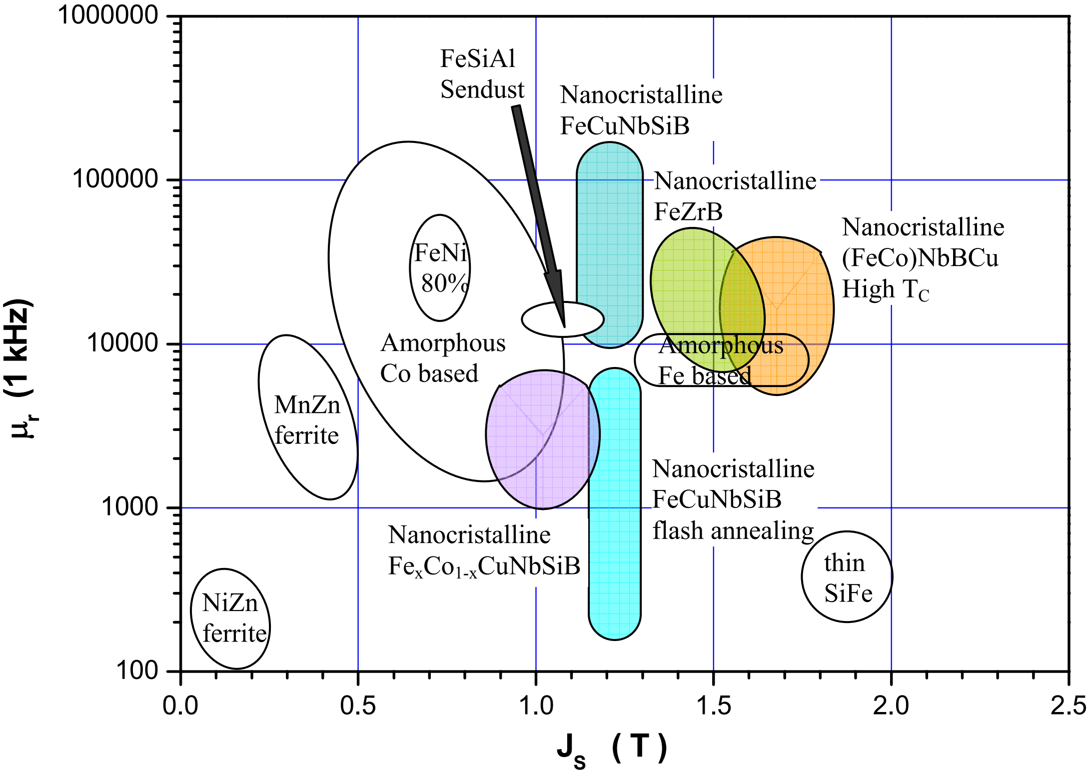

Fig. 11 : general view of soft magnetic materials for medium frequency applications [WAE 06]

* Magnetisation Saturation :

  $J_S \approx$ 1,25 T (Finemet) $J_S \approx$ 1.7 T (Nanoperm) [SUS 91]

* Operating Temperature

  ≈ **150 °C** limited by the Curie Temperature of the residual amorphous phase T_{Cam} (cf. Fig.12)

  ➨ Enhancement of T_{Cam} by partial substitution of Fe by Co in Finemet or Nanoperm (➨ Hitperm) [WIL 99], [MIT 04], [GER 06]

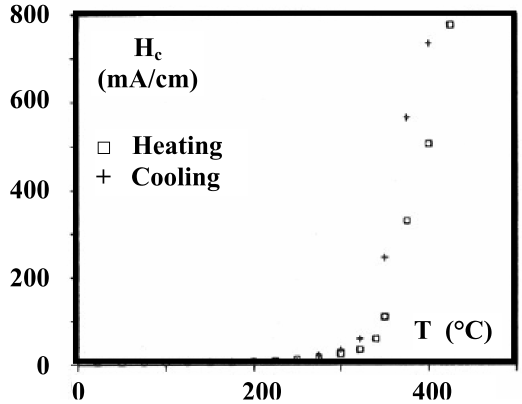

Fig. 12 : Coercivity of Finemet (annealed 1h 540 °C) as a function of temperature measurement [Her 89]

References

[ALV 05] Alves F., Simon F., Kane S. N., Mazaleyrat F., Waeckerle T., Save T., Gupta A., J. Mag. Mag. Mater. 294, 2005, e141

[GEO 06] Geoffroy O., Chazal H., Porteseil J.-L., Waeckerlé T., Alves F., J. Mag. Mag. Mat., 304, 2006, 145

[GER 06] Gercsi Zs., Mazaleyrat F., Varga L. K., J. Mag. Mag. Mat., 302, 2006, 454

[MIT 04] Mitra A., Kim H.-Y., Louzguine D. V., Nishiyama N., Shen B., Inoue A., J. Mag. Mag. Mat., 278, 2004, 299

[NAN 01] Nan CeWen, Huang Jin H., Wenig G. J., J. Mag. Mag. Mat., 233, 2001, 219

[SLA 01] Slawska-Waniewska A., J. Phys. IV France 8, 1998, Pr2-11

[SUS 91] Suzuki K., Makino A., Inoue A., J. Appl. Phys., 70, 1991, 6232

[SUS 98] Suzuki K., Herzer G., Cadogan J.M., J. Mag. Mag. Mat., 177-181, 1998, 949
[SZU 02] Szumiata T., Brzozka K., Gawronski M., Gorka B., Jezuita K., Blazquez-Gamez J. S., Kulik T., Zuberek R., Slawska-Waniewska A., Greneche J.M., J. Mag. Mag. Mater. 250, 2002, 83
[WAE 06] Waeckerle T., Alves F. in "Matériaux magnétiques en génie électrique", Kedous-Lebouc ed., Lavoisier Publishing
[WIL 99] Willard M. A., Huang M.-Q., Laughlin D. E., McHenry M. E., J. Appl. Phys., 85, 1999, 4421
[YOS 88] Yoshizawa Y., Oguma S., Yamauchi K., J. Appl. Phys., 64, 1988, 6044